Mechanisms of substrate selectivity for *Bacillus anthracis* thymidylate kinase

CECILIA CARNROT,[1,3] LIYA WANG,[1] DIMITRI TOPALIS,[2] AND STAFFAN ERIKSSON[1]

[1]Department of Anatomy, Physiology and Biochemistry, The Swedish University of Agricultural Sciences, The Biomedical Centre, S-751 23 Uppsala, Sweden

[2]Laboratoire d'Enzymologie Moléculaire et Fonctionelle, FRE 2852-CNRS-Université, Paris 6, 75005 Paris, France

(RECEIVED December 21, 2007; FINAL REVISION May 23, 2008; ACCEPTED May 28, 2008)

Abstract

Bacillus anthracis is well known in connection with biological warfare. The search for new drug targets and antibiotics is highly motivated because of upcoming multiresistant strains. Thymidylate kinase is an ideal target since this enzyme is at the junction of the de novo and salvage synthesis of dTTP, an essential precursor for DNA synthesis. Here the expression and characterization of thymidylate kinase from *B. anthracis* (*Ba*-TMPK) is presented. The enzyme phosphorylated deoxythymidine-5′-monophosphate (dTMP) efficiently with K_m and V_{max} values of 33 μM and 48 μmol mg^{-1} min^{-1}, respectively. The efficiency of deoxyuridine-5′-monophosphate phosphorylation was ~10% of that of dTMP. Several dTMP analogs were tested, and D-FMAUMP (2′-fluoroarabinosyl-5-methyldeoxyuridine-5′-monophosphate) was selectively phosphorylated with an efficiency of 172% of that of D-dTMP, but L-FMAUMP was a poor substrate as were 5-fluorodeoxyuridine-5′-monophosphate (5FdUMP) and 2′,3′-dideoxy-2′,3′-didehydrothymidine-5′-monophosphate (d4TMP). No activity could be detected with 3′-azidothymidine-5′-monophosphate (AZTMP). The corresponding nucleosides known as efficient anticancer and antiviral compounds were also tested, and D-FMAU was a strong inhibitor with an IC_{50} value of 10 μM, while other nucleosides—L-FMAU, dThd, 5-FdUrd, d4T, and AZT, and 2′-arabinosylthymidine—were poor inhibitors. A structure model was built for *Ba*-TMPK based on the *Staphylococcus aureus* TMPK structure. Docking with various substrates suggested mechanisms explaining the differences in substrate selectivity of the human and the bacterial TMPKs. These results may serve as a start point for development of new antibacterial agents.

Keywords: *Bacillus anthracis*; thymidylate kinase; TMPK; structure model; nucleoside analogs; drug design; FMAU

Bacillus anthracis, a Gram-positive, spore-forming bacterium that causes anthrax, is primarily an animal pathogen but can infect humans and be fatal (Baillie and Read 2001). *B. anthracis* has been used as a potential biological weapon recently in connection with the events of 11 September 2001 (Spencer 2003). At least 17 nations and some autonomous terrorist groups are thought to have or have had offensive biological weapons programs (Inglesby et al. 1999). As such, anthrax is considered a substantial threat.

The regular treatment and prophylaxis of inhalation anthrax rely on antibiotics such as ciprofloxacin, fluoroquinolones, and doxycycline. There are also vaccines available, but they suffer from problems such as relatively

[3]Present address: Department of Cell and Molecular Biology, Uppsala University, PO Box 596, S-751 24 Uppsala, Sweden.

Reprint requests to: Staffan Eriksson, Department of Anatomy, Physiology and Biochemistry, The Swedish University of Agricultural Sciences, The Biomedical Centre, PO Box 575, S-751 23 Uppsala, Sweden; e-mail: staffan.eriksson@afb.slu.se; fax: 46-18-55-07-62.

Abbreviations: AraT, 2′-arabinosylthymidine; AZT, 3′-azidothymidine; AZTMP, 3′-azidothymidine-5′-monophosphate; d4T, 2′,3′-dideoxy-2′,3′-didehydrothymidine; dThd, deoxythymidine; d4TMP, 2′,3′-dideoxy-2′,3′-didehydrothymidine-5′-monophosphate; dTMP, thymidylate, thymidine-5′-monophosphate; dUMP, deoxyuridine-5′-monophosphate; 5-FdUMP, 5-fluorodeoxyuridine-5′-monophosphate; 5-FdUrd, 5-fluorodeoxyuridine; FMAU, 2′-fluoroarabinosyl-5-methyldeoxyuridine; FMAUMP, 2′-fluoroarabinosyl-5-methyldeoxyuridine-5′-monophosphate; TMPK, thymidylate kinase.

Article and publication are at http://www.proteinscience.org/cgi/doi/10.1110/ps.034199.107.

high costs of production and associated transient side effects (Spencer 2003). There is also a danger for upcoming antibiotic resistance and thus a need for new antimicrobial agents with novel targets and mechanisms, which may successfully treat people exposed to or infected with drug-resistant strains of *B. anthracis*.

Most organisms synthesize their DNA precursors by either the de novo or the salvage pathways. The de novo synthesis involves initial synthesis of ribonucleotides, while the salvage pathway reuses nucleosides from DNA degradation. The two pathways vary in activity in different types of cells and during different stages of the cell cycle.

Thymidine 5′-monophosphate kinase (TMPK), expressed in all organisms, catalyzes the transfer of gamma phosphate from ATP to thymidine 5′-monophosphate (dTMP), yielding thymidine 5′-diphosphate (dTDP) and ADP. TMPK is the site where the de novo and salvage pathways meet in dTTP synthesis and, hence, is a good target for drug design.

Most nucleoside analogs used in antiviral and anticancer therapy require stepwise phosphorylation by cellular nucleoside/tide kinases to the respective triphosphates to exert their therapeutic effects. The poor recognition of 3′-azido-dTMP by human TMPK has been a bottleneck for anti-HIV therapy with the therapeutic nucleoside analog 3′-azidothymidine (AZT) (Lavie et al. 1998b). β-L-Nucleosides, such as β-L-(−)-2′,3′-dideoxy-3′-thiacytidine (3TC) and 1-(2′-deoxy-2′-fluoro-β-L-arabinofuranosyl)-5-methyluracil (L-FMAU), have been recognized as potent and selective inhibitors of HIV and hepatitis B virus replication (Balakrishna Pai et al. 1996; Buti and Esteban 2003). Human TMPK selectively phosphorylates the D-enantiomer of dTMP and its analogs, for example, the efficiency for D-FMAUMP phosphorylation was 70-fold higher than that of L-FMAUMP (Hu et al. 2005; Alexandre et al. 2007). The enantioselectivity of nucleoside-activating enzymes most likely have a strong impact on the efficacy and specificity of new antimicrobial agents.

TMPK from *B. anthracis* Sterne strain (AAT52367) (*Ba*-TMPK) shares only 16% sequence identity with human TMPK (hTMPK), while the sequence identity to TMPK of *Staphylococcus aureus* (*Sa*-TMPK) is ~50%. Nevertheless, all known TMPKs showed a highly conserved 3D fold (Lavie et al. 1998a,b; Ostermann et al. 2000; Li de la Sierra et al. 2001; Kotaka et al. 2006). Still, there are (structural) differences that could be used in drug design. For instance, studies with *Mycobacterium tuberculosis* TMPK have led to the identification of potent TMPK inhibitors, which also inhibited the growth of the organism (Vanheusden et al. 2002, 2003; Haouz et al. 2003; Pochet et al. 2003; Fioravanti et al. 2005; Van Daele et al. 2006, 2007).

Here, we describe the expression and characterization of TMPK from *B. anthracis*. Several dTMP analogs used as anticancer and antiviral drugs were tested as substrates. The nucleoside forms of these analogs, that is, 5-FdUrd, AZT, FMAU, and d4T, are used against cancer and viral infections (Furman et al. 1986; Balzarini et al. 1989; Balakrishna Pai et al. 1996; Chu et al. 1998; Marsh and McLeod 2001; Eriksson et al. 2002; Dawson and Lawrence 2004). The specificity of *Ba*-TMPK was investigated using analogs with substitutions at the 5-, 3′-, and 2′-positions, respectively. Structural models of *Ba*-TMPK in complex with several analogs were built based on the 3D structure of *Sa*-TMPK. These results were used to explain the substrate specificity and catalytic rates observed with the enzymes of human and bacterial origin. Specifically, the mechanism involved in stereoisomer selectivity has been addressed by a computational approach. These studies provide a basis for the future design of new agents against *B. anthracis* and related pathogenic bacteria.

Results

Expression and purification

Recombinant *Ba*-TMPK was expressed as an N-terminally His-tagged protein and purified in one step by metal affinity chromatography. Based on SDS-PAGE analysis, the final protein preparation was more than 95% pure (Fig. 1). The amount of recombinant *Ba*-TMPK was estimated to be ~40% of the total protein, and the yield was ≈180 mg of pure protein per liter of culture. Purified *Ba*-TMPK was stable upon repeated freezing and thawing but started to lose activity after 2 d when stored at +4°C. The addition of detergents, for example, Triton X-100, 3-cyclohexylamino-1-propanesulfonic acid, did not affect *Ba*-TMPK activity.

Purified *Ba*-TMPK was analyzed by size exclusion chromatography using a Superdex 200 column. The enzyme eluted as a single peak at a molecular size corresponding to 54 kDa, which suggested that *Ba*-TMPK is a dimer since the calculated molecular weight of the monomer is 26 kDa, including the His-tag.

Substrate specificity

Ba-TMPK was thymidylate-specific and phosphorylated dTMP with high efficiency and to some extent dUMP. All other deoxyribonucleotides and ribonucleotides showed <4% activity (Table 1). dTMP phosphorylation followed the Michaelis-Menten kinetics with a K_m value of 33 μM and a V_{max} value of 48 μmol mg^{-1} min^{-1} of dTDP formed. This resulted in a high k_{cat} value (21 s^{-1}) and catalytic efficiency ($k_{cat}/K_m = 6.4 \times 10^5$ M^{-1} s^{-1}) (Table 2).

In addition to natural nucleoside monophosphates, several dTMP analogs were also tested. FMAUMP, as a racemic mixture, had a slightly lower K_m value (22 μM)

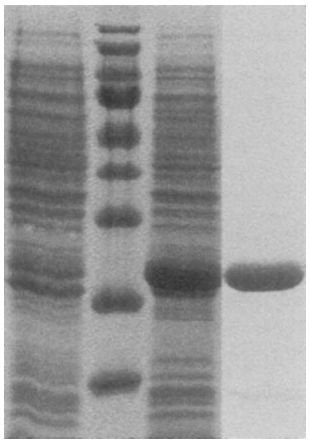

Figure 1. SDS-PAGE of *Ba*-TMPK. (From the *left*) Uninduced cell extract, marker, induced cell extract, purified *Ba*-TMPK. The bands in the marker correspond to ~170, 130, 100, 70, 55, 40, 35, 25, and 15 kDa.

and a lower V_{max} value (13 μmol mg^{-1} min^{-1}), as compared with those of dTMP. The catalytic efficiency (k_{cat}/K_m) of this mixture was threefold lower than that of dTMP. When the individual enantiomers, that is, L- and D-FMAUMP were tested, L-FMAUMP had a K_m value of 167 μM and V_{max} value of 2.3 μmol mg^{-1} min^{-1}, while D-FMAUMP had a K_m value of 4.4 μM and V_{max} value of 11 μmol mg^{-1} min^{-1}, demonstrating that D-FMAUMP was a much better substrate for *Ba*-TMPK with an efficiency of 172% of that of dTMP. 5-FdUMP and d4TMP were poor substrates with high K_m and low V_{max} values. 5-FdUMP had a K_m value about 16 times higher than that of dTMP. The rate-limiting step for d4TMP appeared instead to be the turnover number/rate (k_{cat}), which was more than 50 times lower than that of dTMP (Table 2). AZTMP was also tested, but no activity could be detected (Table 1).

While ATP was used as phosphate donor to mimic physiological conditions, *Ba*-TMPK also accepted dATP as phosphate donor (83% relative activity of ATP), and other natural ribonucleotide and deoxyribonucleotide triphosphates were poor donors. The order of base preference was adenine > cytosine > guanine > uracil > thymine (Fig. 2). Interestingly, the end-product dTTP could be used as phosphate donor, ~3% as compared with ATP.

Some anticancer and antiviral pyrimidine nucleoside analogs were tested for their inhibitory effect on dTMP phosphorylation. Initially, a FMAU preparation, which is a mixture of D- and L-FMAU, was used and found to be the only nucleoside analog that gave a pronounced inhibition with an IC_{50} value of 22 ± 4 μM (Table 3). At 500 μM FMAU, <10% of the activity was found using 10 μM dTMP as substrate (Fig. 3). The individual enantiomers, that is, L- and D-FMAU, were also tested and D-FMAU strongly inhibited *Ba*-TMPK activity with an IC_{50} value of 10 μM, while L-FMAU did not produce any detectable inhibition (Table 3). All the other tested nucleoside analogs were poor inhibitors in the order of d4T > dThd > AZT > AraT > 5-FdUrd. The IC_{50} values for d4T, dThd, and AZT were between 200 and 700 μM, whereas the IC_{50} value of AraT was >1.5 mM. No inhibition was detected with 5-FdUrd (IC_{50} > 4 mM) (Table 3).

The inhibitory effect of D- and L-FMAU toward human TMPK was also examined. L-FMAU did not inhibit hTMPK activity; instead, an unexpected ~30% stimulation was observed. D-FMAU inhibited hTMPK activity only at concentrations >100 μM, and the IC_{50} value was >400 μM.

Structural model of Ba-*TMPK*

We have attempted to crystallize the *Ba*-TMPK but so far without success. Therefore, a structural model was built based on the *Sa*-TMPK structure (pdb code: 2CCJ) (Kotaka et al. 2006), since the two enzymes share ~50% sequence identity. D-dTMP as well as L- and D- FMAUMP were docked in the active site of the *Ba*-TMPK model using the ArgusLab software (www.arguslab.com/arguslab40.htm). L- and D-FMAUMP were also docked into the hTMPK active site with this procedure.

Similar to *Sa*-TMPK, the binding of D-dTMP to *Ba*-TMPK is through a network of hydrogen bonds to the pyrimidine ring involving residues R70, S97, and Q101 (Fig. 4A,E), and the base is stacked by an aromatic residue (Y66), which is also observed in all known TMPK structures (in hTMPK, it corresponds to F72) (Fig. 4C). Q101 interacts with O2 and N3 of the base, and R70 interacts with O4. The 3′-OH group interacts with Y100 via a water molecule. The phosphate group is tightly coordinated by R34, D91, and R92.

Table 1. *Phosphate acceptor specificity of purified recombinant* Ba-*TMPK*

Phosphate acceptor (1 mM)	Activity[a] (%)
dTMP	100
dUMP	10.7
UMP	0.7
dCMP	0.8
CMP	1.0
dGMP	0.8
GMP	0.8
dIMP	0.7
IMP	1.0
dAMP	2.7
AMP	3.7
AZTMP	<0.001

[a]The values are means of three determinations (<20% variation). The specific activity of dTMP was set to 100% (28 μmol mg^{-1} min^{-1}), and 1 mM ATP was used.

Table 2. *Kinetic parameters of purified recombinant* Ba-*TMPK*

Substrate	K_m (μM)	V_{max} (μmol mg^{-1} min^{-1})	k_{cat} (s^{-1})	k_{cat}/K_m (M^{-1} s^{-1})
D-dTMP	33 ± 6	48 ± 2	21	6.4×10^5
D-5-FdUMP	543 ± 4	22 ± 2	9	1.7×10^4
FMAUMP	22 ± 1	13 ± 2	6	2.6×10^5
D-FMAUMP	4.4 ± 0.5	11.2 ± 0.8	5	1.1×10^6
L-FMAUMP	167 ± 10	2.3 ± 0.2	1	5.9×10^3
D-d4TMP[a]	78	0.9	0.4	4.8×10^3

The values are means ± SD of three to four determinations. 1 mM ATP was used as phosphate donor. The k_{cat} values were calculated based on a subunit molecular weight of 26 kDa.
[a]Results from one experiment.

The binding of L-FMAUMP and D-FMAUMP to *Ba*-TMPK is shown in Figure 4B. The pyrimidine ring is bound in the same fashion as for D-dTMP. Two additional hydrogen bonds are predicted between the 2′-fluorine of D-FMAUMP and the amino group of Q101, and between the O1′ from the arabinosyl moiety and the hydroxyl group from Y66. Binding of the 2′-fluorine and O1′ with Q101 and Y66, respectively, may be responsible for the increased binding affinity of D-FMAUMP to *Ba*-TMPKs. The stacking interaction is also enhanced because the base is closer to Y66. Altogether, this may account for the increased binding affinity for D-FMAUMP ($K_M^{(D\text{-FMAUMP})} =$ 4.4 μM as compared with the K_M for D-dTMP = 33 μM). The binding of the phosphate groups is different as a hydrogen bond appears between E8 and the arabinose derivatives. The interaction between D91 and the phosphate moiety is missing as compared with D-dTMP (Fig. 4A). In the case of D-FMAUMP, R92 provides most likely two H-bonds with the phosphate group, whereas this interaction is missing in L-FMAUMP (Fig. 4B). This may explain why D-FMAUMP is a better substrate ($K_M^{(D\text{-FMAUMP})} = 4.4$ μM and $k_{cat} = 6\ s^{-1}$) than its L-enantiomer ($K_M^{(D\text{-FMAUMP})} = 167$ μM and $k_{cat} = 1.0\ s^{-1}$).

In the case of hTMPK, Y151, H69, and R76 are the main residues involved in the H-bond network to the pyrimidine ring. The 3′-OH of D-dTMP is bound to residue Q157 via a water molecule in the LID domain, and D15 and S20 from the P-loop play a key role in D-dTMP phosphate binding (Alexandre et al. 2007). The binding of the pyrimidine ring of D- and L-FMAUMP is similar to that of D-dTMP. However, R97 is able to bind both the 2′-F and 3′-OH of the arabinose of D-FMAUMP, which enhances its binding affinity to hTMPK. The phosphate moiety is closely bound to R45 instead of D15 and S20, explaining the reduced catalytic activity of D-FMAUMP as compared with D-dTMP. In case of L-FMAUMP, the 3′-OH is bound to the core domain via R45 but not to the LID domain (Q157 via a water molecule) as observed with the D-dTMP (Fig. 4C,D).

L- and D-FMAU were also docked onto *Ba*-TMPK active site using the same conditions as for the monophosphate forms (Fig. 4F). L-FMAU bound to the enzyme in a different fashion from the monophosphate counterpart. The pyrimidine ring is weakly bound to the active site. Only the O4 atom interacts with S97, while O2 and N3 are not involved in H-bond interactions. O1′ is maintained by R92, and the 5′-OH is interacting via H-bonds to R34 and D91. This weak binding may explain the high IC_{50} value observed (>5 mM). D-FMAU, on the other hand, is tightly bound to the active site since the base is stacked to Y66 very well, and N3 and O4 participate with H-bond interacting with R70, S97, and Q101. In addition, R92 interacts with the 2′-fluorine group and 3′-OH via two hydrogen bonds, and R34 is close enough to 5′-OH to establish two H-bonds. These interactions may explain why D-FMAU is an efficient inhibitor of *Ba*-TMPK ($IC_{50} = 10$ μM), although it lacks a 5′-phosphate group.

Discussion

Targeting thymidylate biosynthesis is an efficient way to block DNA synthesis, eventually leading to cell death. Because of its unique position in both the de novo and the salvage synthesis of dTTP, *Ba*-TMPK is a promising drug target for antibiotic development. Therefore, we have characterized *Ba*-TMPK with focus on its substrate specificity to get a deeper understanding of the enzyme and substrate interactions. The acquired knowledge concerning *Ba*-TMPK will also help in understanding the functional differences and similarities between TMPKs from other species.

All known TMPKs are dimers, and a classification of TMPKs has been proposed with respect to the location of specific residues in the active site (Lavie et al. 1998b). Class I TMPKs, for example, human and yeast TMPK, have an arginine in the P-loop interacting with the phosphate donor, while class II TMPKs, for example, *Escherichia coli*

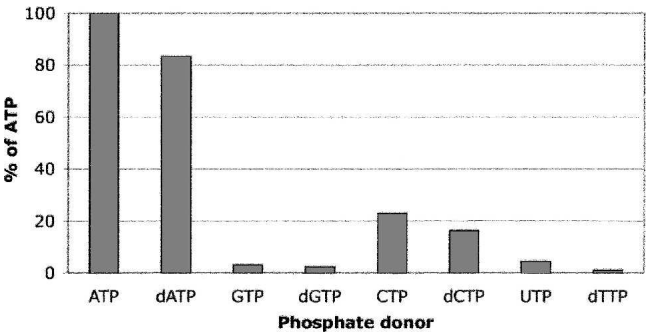

Figure 2. Phosphate acceptor specificity of purified recombinant *Ba*-TMPK. The phosphorylation rate with ATP was set to 100%. Phosphate donors and dTMP were 2 mM and 100 μM, respectively.

Table 3. *IC_{50} values of nucleosides as inhibitors with recombinant* Ba-*TMPK*

Compound	IC_{50} (μM)
dThd	438 ± 7
5-FdUrd	>4000
FMAU	22 ± 4
L-FMAU	>5000
D-FMAU	10 ± 2
d4T	244 ± 11
AZT	702 ± 3
AraT	>1500

The values are means ± SD of three to four determinations. 10 μM dTMP was used as substrate, and 1 mM ATP was used as phosphate donor.

and *Staphylococcus aureus*, instead have a glycine in the same position. Additionally, class II enzymes have interacting basic residues, mostly arginines, in the LID region. *Ba*-TMPK was shown to be a dimer in this study and had the sequence characteristics of a class II TMPK.

The phosphate donor study showed that ATP/dATP and to a lower extent CTP/dCTP were accepted by *Ba*-TMPK, similar to *Streptococcus pneumoniae* TMPK (*Sp*-TMPK) (Petit and Koretke 2002), whereas other TMPKs use a broader set of phosphate donors. The *Ba*- and *Sp*-TMPK sequences do not show any special feature or motif at the amino acid level that could explain their narrow phosphate donor specificity. An alignment of TMPK sequences from eukaryotes, bacteria, and archaea demonstrates large sequence diversity between different organisms (Li de la Sierra et al. 2001).

Ba-TMPK was strictly thymidylate-specific and had low affinity for dUMP, in line with earlier publications with other TMPKs (Jong and Campbell 1984; Petit and Koretke 2002; Vanheusden et al. 2002). An exception is *Vaccinia virus* TMPK (vv-TMPK), which also phosphorylates dGMP, although at a fourfold lower rate (Topalis et al. 2005). The poor activity with dUMP for TMPK of *B. anthracis* and other organisms could be a safety mechanism to prevent a buildup of dUTP, which may cause replication mistakes. The very high K_m value and almost 40 times lower efficiency for 5-FdUMP (compared to dTMP) further showed the sensitivity of *Ba*-TMPK for modifications at the 5 position of the base. In the modeled *Ba*-TMPK structure, the pyrimidine ring is located in the middle of a hydrophobic pocket delineated by five nonpolar residues (Y66, P36, H73, F93, and Y100) (Fig. 4A). The 5-methyl group contributes to the stability of the substrate/enzyme complex. Substitutions such as H (dUMP) or F (5FdUMP) are not likely to fit in this hydrophobic pocket. Therefore, dUMP and 5FdUMP are poor substrates.

The base moiety plays a key role in substrate recognition of *Ba*-TMPK, but the 2′- and 3′-positions on the sugar are also very important as demonstrated in this study. UMP is 10 times less efficient than dUMP. Thus, the 2′-position of the ribose does not tolerate any substitutions larger than a hydrogen atom. Concerning the arabinose derivatives, that is, FMAUMP, a 2′-arabinosyl fluoro substitution is advantageous since FMAUMP had a lower K_m value (22 μM) as compared with dTMP (33 μM) and a catalytic efficiency ~40% of that of dTMP. When the individual enantiomers were tested, it turned out that D-FMAUMP was the selective substrate but not the corresponding L-form. D-FMAUMP was the most efficient substrate and a highly promising substrate analog. As observed in the modeled D- and L-FMAUMP/*Ba*-TMPK binary complexes, the binding of the phosphate group to the enzyme is similar with E8 involved in both cases. It is the interactions with the sugar moiety in the two compounds that differ. The hydrogen bonding of the 2′-F of the arabinosyl moiety in D-FMAUMP to residue Q101 and O′1 to the hydroxyl group of residue Y66 contributed to its high affinity for the enzyme.

The 3′-position modifications are, in comparison with the 2′-position, more restricted since the tested 3′-analogs, d4TMP and AZTMP, were poor substrates for *Ba*-TMPK, as well as the corresponding nucleoside analogs d4T and AZT were poor inhibitors. The efficiency for d4TMP was <1% of that of dTMP, and AZTMP had no detectable activity. These results are in accordance with previous studies with hTMPK, *Mt*-TMPK, and vv-TMPK (Munier-Lehmann et al. 2001; Ostermann et al. 2003; Hu et al. 2005; Topalis et al. 2005). The lack of phosphorylation of AZTMP by *Ba*-TMPK could be an explanation for the poor growth inhibition of *B. anthracis* with AZT. AZT is readily phosphorylated by *Ba*-TK (Carnrot et al. 2006), but if AZTMP cannot be further phosphorylated by *Ba*-TMPK, for example, it will not reach its active form—AZTTP.

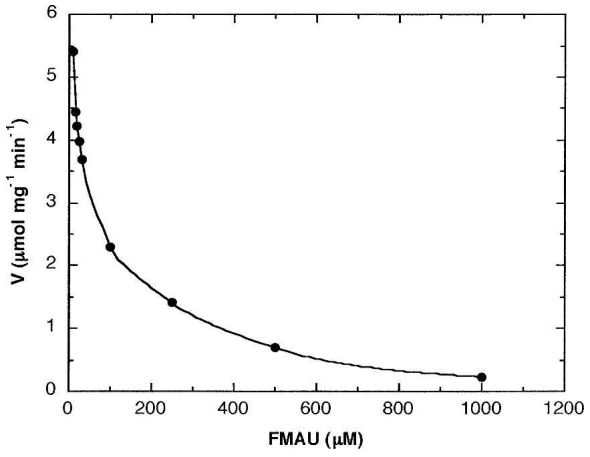

Figure 3. Activity of *Ba*-TMPK with dTMP in the presence of FMAU, 10 μM dTMP, and 1 mM ATP were used together with different concentrations of FMAU ranging from 10 to 1000 μM. The experiment was done three times, and the IC_{50} value was calculated to be 22 ± 4 μM.

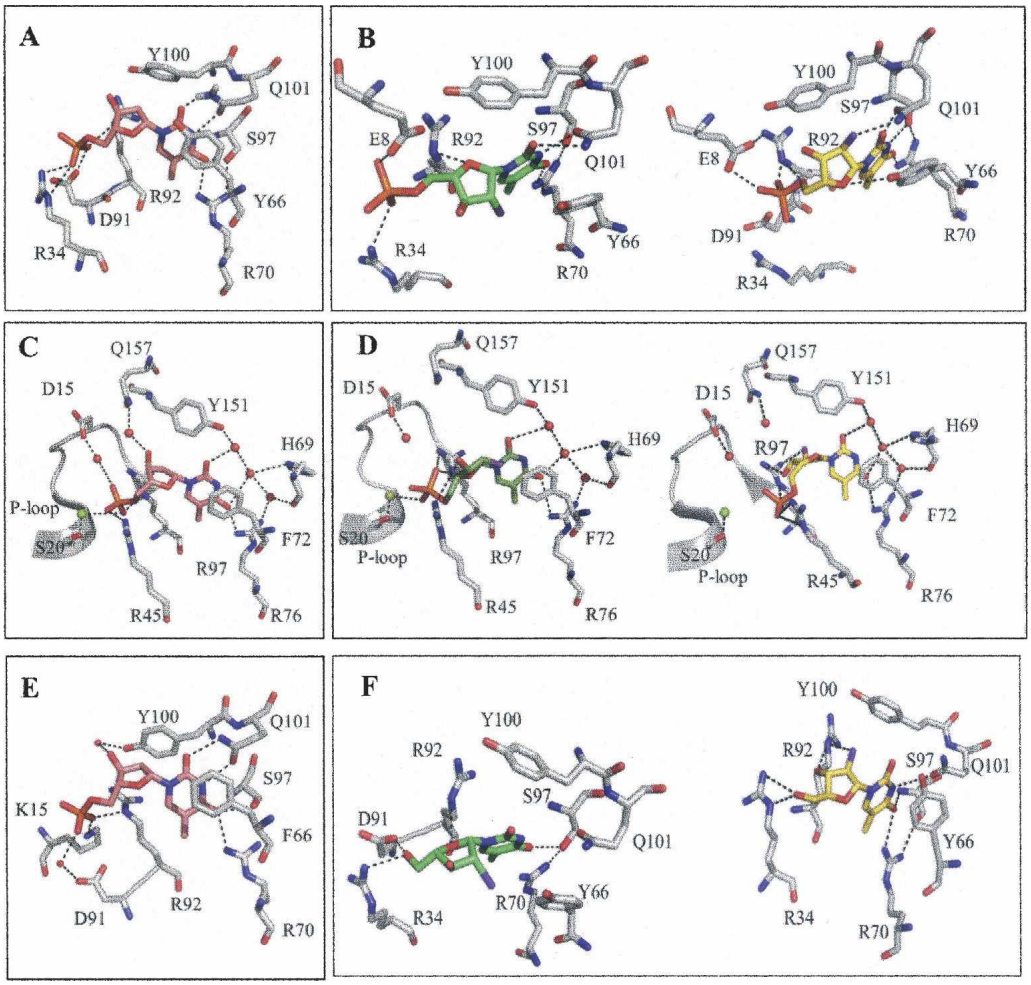

Figure 4. Molecular docking of D-dTMP (in pink), L-FMAUMP (in green), and D-FMAUMP (in yellow) in the active site of *Ba*-TMPK and *h*TMPK. (*A*) D-dTMP complexed with *Ba*-TMPK; (*B*) L-FMAUMP and D-FMAUMP in complex with *Ba*-TMPK. Fluorine atom is colored purple. (*C*) D-dTMP in *h*TMPK active site. (*D*) L-FMAUMP and D-FMAUMP in complex with *h*TMPK. Magnesium ion is represented by a green sphere and water molecules are in red. (*E*) D-dTMP in *Sa*TMPK active site. (*F*) L-FMAU (green) and D-FMAU (yellow) in the active site of *Ba*-TMPK.

Therefore, with AZT in the growth media, the effective dose (ED_{50}) is high, >1 mM (Carnrot et al. 2006).

The enantioselectivity of hTMPK also favors the D-configuration of dTMP and its analogs as shown in recent studies with D- and L-dTMP as well as with D- and L-FMAUMP (Hu et al. 2005; Alexandre et al. 2007). The kinetic data show that D-FMAUMP ($K_m = 6$ μM and $V_{max} = 2.6$ μmol min^{-1} mg^{-1}) is a much better substrate than L-FMAUMP ($K_m = 21.7$ μM and $V_{max} = 0.12$ μmol min^{-1} mg^{-1}) (Hu et al. 2005). The selectivity of D-FMAUMP over L-FMAUMP is explained here in the modeled D- and L-FMAUMP/hTMPK complex. Both the 2′-F and 3′-OH of the D-FMAUMP interact with residue R97, but this is not the case with the L-configuration.

When nucleosides were tested as inhibitors toward *Ba*-TMPK, FMAU had an IC_{50} value that was almost identical to the K_m value of FMAUMP, and of the two enantiomers, it was D-FMAU that inhibited the enzyme but not L-FMAU. These results strongly indicate that the substrate binding affinity is determined to a large extent by the nucleoside moiety and that the 5′-phosphate played a minor role in the case of D-FMAU and *Ba*-TMPK. This hypothesis is strengthened by docking of the two nucleosides in the active site of the *Ba*-TMPK model structure (Fig. 4F). However, as shown here, this was not the case with hTMPK since D-FMAU was not an inhibitor and L-FMAU instead apparently stimulated the hTMPK activity. These significant differences between human and bacterial TMPKs, which was also observed with the *M. tuberculosis* enzyme (Pochet et al. 2003), should be investigated further.

The phosphate group of dTMP provides much of the binding energy in catalysis carried out by TMPKs. An

ideal drug candidate should not carry a charged group because of its difficulties in uptake through cell membranes. The differences observed in the inhibitory effect of D- and L-FMAU on *Ba*-TMPK and human TMPK suggest that there are differences in the binding mode of these nucleoside analogs to the active site of the enzymes. This difference may be advantageous in designing specific nonsubstrate inhibitors, for example, nucleoside analogs for *Ba*-TMPK with little or no effect on hTMPK. The development of narrow-spectrum rather than broad-spectrum antibiotics may reduce the risk of transfer of drug resistance between different bacterial species. This study provides a good starting point for future development of antibiotics against *B. anthracis* and other pathogenic bacteria such as *S. aureus*.

Materials and Methods

Materials

[2′,3′-^{3}H]Thymidine-5′-monophosphate ([^{3}H]dTMP; 34.6 Ci/mmol), (1-β-D)-2′-fluoroarabinosyl-5-methyldeoxyuridine (D-FMAU), and 2′,3′-dideoxy-2′,3′-didehydrothymidine-5′-monophosphate (d4TMP) were purchased from Moravek Biochemicals Inc. 5-Fluorodeoxyuridine (5-FdUrd), 5-fluorodeoxyuridine-5′-monophosphate (5-FdUMP), 3′-azidothymidine (AZT), 2′,3′-didehydrothymidine (d4T), 2′-arabinosylthymidine (AraT), deoxythymidine (dThd), and dTMP were from Sigma-Aldrich. 2′-Fluoroarabinosyl-5-methyldeoxyuridine (FMAU), a mixture of the D- and L-form, was a gift from J. Fox (Memorial Sloan Kettering Cancer Institute, New York). 3′-Azidothymidine-5′-monophosphate (AZTMP) was a gift from W. Tjarks (College of Pharmacy and Center for Microbial Interface Biology, Ohio State University). L-FMAU was kindly provided by Hee-Won Yoo (Bukwang Pharm. Co., Ltd). The FMAU 5′-monophosphates were synthesized enzymatically as described previously (Jacobsson et al. 1998).

Cloning and expression of the B. anthracis tmpk *gene*

The plasmid DNA containing the *B. anthracis* Sterne strain (34F2) *tmpk* gene in the pCR4-TOPO vector (Invitrogen) was kindly provided by A.J. Phipps (Department of Veterinary Biosciences, The Center for Microbial Interface Biology, Ohio State University, Columbus) (Byun et al. 2007). The *tmpk* gene was then subcloned into the pET-14b expression vector and transformed into the chemical competent *E. coli* strain, *BL21(DE3) pLysS* (Novagen), as previously described (Carnrot et al. 2006). The bacteria were cultured as previously described at 37°C to an OD_{600} of 0.6. Recombinant *Ba*-TMPK was expressed by induction for 6 h with 0.4 mM IPTG at 25°C. Purification of recombinant *Ba*-TMPK was done as previously described (Carnrot et al. 2003), and the enzyme was analyzed with SDS-PAGE. Human TMPK was expressed and purified as previously described (Alexandre et al. 2007).

Molecular weight estimation

Purified recombinant *Ba*-TMPK was applied to a Superdex 200 column (Amersham Biosciences, GE Healthcare) attached to an FPLC instrument (Amersham Biosciences, GE Healthcare). The column was equilibrated with 20 mM Tris-HCl pH 7.6, 0.2 M NaCl, 1 mM DTT, and 2 mM $MgCl_2$. The column was initially calibrated with blue dextran (2000 kDa), alcohol dehydrogenase (150 kDa), bovine serum albumin (66 kDa), ovalbumin (42 kDa), and cytochrome *c* (12.4 kDa; Sigma-Aldrich). The molecular size of active *Ba*-TMPK was estimated by using the calibration curve.

Enzyme assays

TMPK activity was followed by the ADP production in a coupled enzyme system with pyruvate kinase and lactate dehydrogenase (Blondin et al. 1994). The standard reaction mixture contained 50 mM Tris-HCl pH 7.6, 2 mM $MgCl_2$, 1 mM ATP, 5 mM DTT, 1 mM phosphoenolpyruvate, 2 units/mL pyruvate kinase, 2 units/mL lactate dehydrogenase, 100 μM NADH, and a final concentration of 0.5 μg/mL *Ba*-TMPK in a total volume of 1 mL. The reaction was performed at 37°C with a Cary 3 spectrophotometer (Varian Techtron). Phosphate donor specificity was determined by using 100 μM [^{3}H]dTMP as substrate as described previously (Wang 2007). The reaction products were separated by thin layer chromatography and quantified by liquid scintillation counting (Beckman Coulter LS 6500).

The mean and the standard deviation (SD) were calculated, and the IC_{50} values were defined as the concentration of an inhibitor that decreases the enzyme maximum velocity with 50%. Kinetic parameters were calculated by using the Michaelis-Menten equation in KALEIDAGRAPH (Synergy Software).

Modeling studies

D- and L-FMAUMP as well as the corresponding nucleosides were drawn with Molsoft (http://www.molsoft, 2D to 3D converter) and Smiles Translator (http://cactus.nci.nih.gov/services/translate/) to produce the pdb file. The conformation of the sugar ring was checked by visualizing the molecules within the PyMOL graphic system (DeLano Scientific) and, if necessary, modified to the β-L configuration, as desired. Docking of the L- and D-FMAUMP and L- and D-FMAU and D-dTMP was performed using ArgusLab software (www.arguslab.com/arguslab40.htm). The binding site was defined from the coordinates of the ligand in the original PDB files 1E2D for *h*TMPK and a model of *Ba*-TMPk based on *Sa*-TMPK (pdb code: 2CCJ). Docking precision was set to ''high,'' and the ''flexible ligand docking'' mode was used for each docking run. Resulting complexes were visualized with the PyMOL graphic system.

Acknowledgments

This work was supported by grants from the Swedish Research Council for the Environment, Agricultural Sciences and Spatial Planning (FORMAS), and the Swedish Research Council. We thank Dominique Devill-Bonne for providing us with the human TMPK plasmid.

References

Alexandre, J.A.C., Roy, B., Topalis, D., Pochet, S., Périgaud, C., and Deville-Bonne, D. 2007. Enantioselectivity of human AMP, dTMP and UMP-CMP kinases. *Nucleic Acids Res.* **35:** 4895–4904.

Baillie, L. and Read, T. 2001. *Bacillus anthracis*, a bug with attitude! *Curr. Opin. Microbiol.* **4:** 78–81.

Balakrishna Pai, S., Liu, S.H., Zhu, Y.L., Chu, C.K., and Cheng, Y.C. 1996. Inhibition of hepatitis B virus by a novel L-nucleoside, 2′-fluoro-5-methyl-β-L-arabinofuranosyl uracil. *Antimicrob. Agents Chemother.* **40:** 380–386.

Balzarini, J., Herdewijn, P., and De Clercq, E. 1989. Differential patterns of intracellular metabolism of 2′,3′-didehydro2′,3′-dideoxythymidine and 3′-azido-2′,3′-dideoxythymidine, two potential anti-human immunodeficiency virus compounds. *J. Biol. Chem.* **264:** 6127–6133.

Blondin, C., Serina, L., Wiesmuller, L., Gilles, A., and Barzu, O. 1994. Improved spectrophotometric assay of nucleoside monophosphate kinase activity using the pyruvate kinase/lactate dehydrogenase coupling system. *Anal. Biochem.* **220:** 219–221.

Buti, M. and Esteban, R. 2003. Entecavir, FTC, L-FMAU, LdT and others. *J. Hepatol.* **39:** S139–S142.

Byun, Y., Carnrot, C., Vogel, S., Usova, E., Phipps, A., Eriksson, S., and Tjarks, W. 2007. Synthesis and biological evaluation of inhibitors of thymidine kinase and thymidine monophosphate kinase from *Bacillus anthracis*. *Nucleosides Nucleotides Nucleic Acids* **27:** 244–260.

Carnrot, C., Wehelie, R., Eriksson, S., Bölske, G., and Wang, L. 2003. Molecular characterization of thymidine kinase from *Ureaplasma urealyticum*: Nucleoside analogues as potent inhibitors of *mycoplasma* growth. *Mol. Microbiol.* **50:** 771–780.

Carnrot, C., Vogel, S., Byun, Y., Wang, L., Tjarks, W., Eriksson, S., and Phipps, A. 2006. Evaluation of thymidine kinase as a potential target for development of nucleoside analogs against *Bacillus anthracis*. *Biol. Chem.* **387:** 1575–1581.

Chu, C.K., Boudinot, F.D., Peek, S.F., Hong, J.H., Choi, Y., Korba, B.E., Gerin, J.L., Cote, P.J., Tennant, B.C., and Cheng, Y.C. 1998. Preclinical investigation of L-FMAU as an anti-hepatitis B virus agent. *Antivir. Ther.* (Suppl 3) **3:** 113–121.

Dawson, L. and Lawrence, T. 2004. The role of radiotherapy in the treatment of liver metastases. *Cancer J.* **10:** 139–144.

Eriksson, S., Munch-Petersen, B., Johansson, K., and Eklund, H. 2002. Structure and function of cellular deoxyribonucleoside kinases. *Cell. Mol. Life Sci.* **59:** 1327–1346.

Fioravanti, E., Adam, V., Munier-Lehmann, H., and Bourgeois, D. 2005. The crystal structure of *Mycobacterium tuberculosis* thymidylate kinase in complex with 3′-azidodeoxythymidine monophosphate suggests a mechanism for competitive inhibition. *Biochemistry* **44:** 130–137.

Furman, P., Fyfe, J., St. Clair, M., Weinhold, K., Rideout, J., Freeman, G., Nusinoff Lehrmann, S., Bolognesi, D., Broder, S., Mitsuya, H., et al. 1986. Phosphorylation of 3′-azido-3′-deoxythymidine and selective interaction of the 5′-triphosphate with human immunodeficiency virus reverse transcriptase. *Proc. Natl. Acad. Sci.* **83:** 8333–8337.

Haouz, A., Vanheusden, V., Munier-Lehmann, H., Froeyen, M., Herdewijn, P., Van Calenbergh, S., and Delarue, M. 2003. Enzymatic and structural analysis of inhibitors designed against *Mycobacterium tuberculosis* thymidylate kinase. *J. Biol. Chem.* **278:** 4963–4971.

Hu, R., Li, L., Degrève, B., Dutschman, G., Lam, W., and Cheng, Y.-C. 2005. Behavior of thymidylate kinase toward monophosphate metabolites and its role in the metabolism of 1-(2′-deoxy-2′-fluoro-b-L-arabinofuranosyl)-5-methyluracil (Clevudine) and 2′,3′-didehydro-2′,3′-dideoxythymidine in cells. *Antimicrob. Agents Chemother.* **49:** 2044–2049.

Inglesby, T., Henderson, D., Bartlett, J., Ascher, M., Eitzen, E., Friedlander, A., Hauer, J., McDade, J., Osterholm, M., O'Toole, T., et al. 1999. Anthrax as a biological weapon: Medical and public health management. Working group on civilian Biodefense. *JAMA* **281:** 1735–1745.

Jacobsson, B., Britton, S., Tornevik, Y., and Eriksson, S. 1998. Decrease in thymidylate kinase activity in peripheral blood mononuclear cells from HIV-infected individuals. *Biochem. Pharmacol.* **56:** 389–395.

Jong, A. and Campbell, J. 1984. Characterization of *Saccharomyces cerevisiae* thymidylate kinase, the CDC8 gene product. *J. Biol. Chem.* **259:** 14394–14398.

Kotaka, M., Dhaliwal, B., Ren, J., Nichols, C.E., Angell, R., Lockyer, M., Hawkins, A.R., and Stammers, D.K. 2006. Structures of *S. aureus* thymidylate kinase reveal an atypical active site configuration and an intermediate conformational state upon substrate binding. *Protein Sci.* **15:** 774–784.

Lavie, A., Konrad, M., Brundiers, R., Goody, R., Schlichting, I., and Reinstein, J. 1998a. Crystal structure of yeast thymidylate kinase complexed with the bisubstrate inhibitor P^1-(5′-adenosyl) P^5-(5′-thymidyl) pentaphosphate (TP_5A) at 2.0 Å resolution: Implications for catalysis and AZT activation. *Biochemistry* **37:** 3677–3686.

Lavie, A., Ostermann, N., Brundiers, R., Goody, R.S., Reinstein, J., Konrad, M., and Schlichting, I. 1998b. Structural basis for efficient phosphorylation of 3′-azidothymidine monophosphate by *Escherichia coli* thymidylate kinase. *Proc. Natl. Acad. Sci.* **95:** 14045–14050.

Li de la Sierra, I., Munier-Lehmann, H., Gilles, A.M., Barzu, O., and Delarue, M. 2001. X-ray structure of TMP kinase from *Mycobacterium tuberculosis* complexed with TMP at 1.95 Å resolution. *J. Mol. Biol.* **311:** 87–100.

Marsh, S. and McLeod, H. 2001. Thymidylate synthase pharmacogenetics in colorectal cancer. *Clin. Colorectal Cancer* **1:** 175–178.

Munier-Lehmann, H., Chaffotte, A., Pochet, S., and Labesse, G. 2001. Thymidylate kinase of *Mycobacterium tuberculosis*: A chimera sharing properties common to eukaryotic and bacterial enzymes. *Protein Sci.* **10:** 1195–1205.

Ostermann, N., Schlichting, I., Brundiers, R., Konrad, M., Reinstein, J., Veit, T., Goody, R., and Lavie, A. 2000. Insights into the phosphoryltransfer mechanism of human thymidylate kinase gained from crystal structures of enzyme complexes along the reaction coordinate. *Structure* **8:** 629–642.

Ostermann, N., Segura-Pena, D., Meier, C., Veit, T., Monnerjahn, C., Konrad, M., and Lavie, A. 2003. Structures of human thymidylate kinase in complex with prodrugs: Implications for the structure-based design of novel compounds. *Biochemistry* **42:** 2568–2577.

Petit, C. and Koretke, K. 2002. Characterization of *Streptococcus pneumoniae* thymidylate kinase: Steady-state kinetics of the forward reaction and isothermal titration calorimetry. *Biochem. J.* **363:** 825–831.

Pochet, S., Dugué, L., Labesse, G., Delepierre, M., and Munier-Lehmann, H. 2003. Comparative study of purine and pyrimidine nucleoside analogues acting on the thymidylate kinases of *Mycobacterium tuberculosis* and of humans. *ChemBioChem* **4:** 742–747.

Spencer, R. 2003. *Bacillus anthracis*. *J. Clin. Pathol.* **56:** 182–187.

Topalis, D., Collinet, B., Gasse, C., Dugué, L., Balzarini, J., Pochet, S., and Deville-Bonne, D. 2005. Substrate specificity of vaccinia virus thymidylate kinase. *FEBS J.* **272:** 6254–6265.

Van Daele, I., Munier-Lehmann, H., Hendrickx, P.M.S., Marchal, G., Chavarot, P., Froeyen, M., Qing, L., Martins, J.C., and Van Calenbergh, S. 2006. Synthesis and biological evaluation of bicyclic nucleosides as inhibitors of *M. tuberculosis* thymidylate kinase. *ChemMedChem* **1:** 1081–1090.

Van Daele, I., Munier-Lehmann, H., Froeyen, M., Balzarini, J., and Van Calenbergh, S. 2007. Rational design of 5′-thiourea-substituted α-thymidine analogues as thymidine monophosphate kinase inhibitors capable of inhibiting mycobacterial growth. *J. Med. Chem.* **50:** 5281–5292.

Vanheusden, V., Munier-Lehmann, H., Pochet, S., Herdewijn, P., and Van Calenbergh, S. 2002. Synthesis and evaluation of thymidine-5′-*O*-monophosphate analogues as inhibitors of *Mycobacterium tuberculosis* thymidylate kinase. *Bioorg. Med. Chem. Lett.* **12:** 2695–2698.

Vanheusden, V., Van Rompay, A., Munier-Lehmann, H., Pochet, S., Herdewijn, P., and Van Calenbergh, S. 2003. Thymidine and thymidine-5′-*O*-monophosphate analogues as inhibitors of *Mycobacterium tuberculosis* thymidylate kinase. *Bioorg. Med. Chem. Lett.* **13:** 3045–3048.

Wang, L. 2007. The role of Ureaplasma nucleoside monophosphate kinases in the synthesis of nucleoside triphosphates. *FEBS J.* **274:** 1983–1990.